scientific reports

Check for updates

OPEN

CAPZB mRNA is a novel biomarker for cervical high-grade squamous lesions

Xia Cai[1], Wanqiu Huang[2], Jian Huang[2], Xiuxiang Zhu[1], Lifeng Wang[1], Ziyin Xia[1] & Ling Xu[1]✉

This study aimed to evaluate the potential of capping protein (actin filament) muscle Z-line subunit β (CAPZB) messenger ribonucleic acid (mRNA) levels as a biomarker for distinguishing low-grade squamous intraepithelial lesions of the cervix (LSIL) from high-grade squamous intraepithelial lesions of the cervix (HSIL). We collected a total of 166 cervical exfoliated cells and divided them into five groups based on histopathological results. Each sample was divided into two portions, one for fluorescence in situ hybridization (FISH) detection and the other for bisulfite sequencing polymerase chain reaction (BSP) detection. We found that FISH detection of CAPZB mRNA mean fluorescence intensity (MFI) and BSP detection of CAPZB deoxyribonucleic acid (DNA) percentage of methylation rate (PMR) performed as biomarkers for distinguishing HSIL from LSIL, with an area under the receiver operating characteristic curve (AUC), sensitivity, specificity and cut-off value of 0.893, 81.25%, 80.39% and 0.616, 0.794, 64.06%, 81.37% and 0.454, respectively. Furthermore, FISH detection of CAPZB mRNA exhibited a greater AUC (0.893) for the detection of HSIL than the CAPZB DNA methylation method (0.794), indicating the CAPZB mRNA levels can be used as a biomarker for assessing cervical lesions.

Keywords CAPZB, Messenger RNA, Fluorescence in situ hybridization, DNA methylation, Cervical cancer

According to statistics, there were approximately 661,021 new cases and 348,189 deaths from cervical cancer (CC) worldwide in 2022[1] and the age of onset is decreasing in China[2]. Persistent infection with high-risk human papillomavirus (HR-HPV) is the main cause of cervical cancer[3]. Currently, the two mainstream screening and diagnosis methods for cervical cancer in China are the Thin-Prep cytology test (TCT) and HPV testing[4]. While the TCT has high specificity but low sensitivity, HPV testing has high sensitivity but low specificity[5,6]. Therefore, it is crucial to update and improve screening methods to accurately detect high-grade squamous intraepithelial lesions of the cervix (HSIL) and higher stages of cervical lesions to prevent disease progression.

Deoxyribonucleic acid (DNA) methylation, a type of epigenetic regulation, is involved in the abnormal expression of tumour suppressor genes and is another important cause of cervical cancer[7,8]. In a previous study, our research group employed the Illumina HumanMethylation450 BeadChip method to conduct methylation sequencing on different cervical tissues. Based on the β values from the data, intergroup selection was performed, resulting in the identification of five genes. Real-time quantitative reverse transcription polymerase chain reaction (RT−qPCR) was used to measure the expression of these genes in various cervical lesions, revealing that the capping protein (actin filament) muscle Z-line subunit β (CAPZB) exhibited the greatest differences among the groups. The screening process of the investigated gene was shown in Supplementary Figures S1 and S2.

This gene may serve as a target for the early detection of cervical lesions and late-stage cervical cancer treatment. Capping protein (CP), which was initially identified and purified in muscle, plays a crucial role in controlling cell shape and movement[9]. CP consists of α and β subunits, and the β subunit, CAPZB, is expressed in normal tissues (lymphocytes, bladder epithelium, placenta) as well as certain tumour tissues[10]. Studies have shown that CAPZB is associated with cell growth and motility in epithelioid sarcoma; autoimmune diseases such as Crohn's disease and lichen planus; neurodegenerative diseases such as Alzheimer's disease; and several types of cancer such as lung and ovarian cancer[11–14]. However, the role of CAPZB in cervical lesions is still unclear.

Currently, there are various methods for methylation testing, and the most widely used method is based on DNA treated with bisulfite[15], which also has limitations, such as the high temperature and high salt conditions during conversion, which can cause DNA fragmentation and loss, and the critical design of primers[15–17].

[1]Department of Gynaecology, Minhang Hospital, Fudan University, Shanghai 201199, China. [2]Key Laboratory of Systems Biomedicine (Ministry of Education), Shanghai Centre for Systems Biomedicine, Shanghai Jiao Tong University, Shanghai 200240, China. ✉email: xu_ling@fudan.edu.cn

Researchers have found that messenger ribonucleic acid (mRNA) carries genetic information and accurately reflects gene transcription activity. mRNA acts as a template for protein synthesis, determining the arrangement of amino acids in the polypeptide chain[18]. In other diseases, mRNA levels of particular genes have been used as diagnostic and prognostic biomarkers[19–21]. Furthermore, whether the mRNA level of the CAPZB gene can be used as a biomarker for cervical lesion diagnosis is unknown. Therefore, this study aimed to explore the feasibility of using CAPZB mRNA levels for cervical lesion screening.

Results

Clinical characteristics of the study population

Table 1 summarized the detailed clinical characteristics of the study population. A total of 166 cervical cell samples were analysed: the normal group and the CC group had 30 samples each (18.07%), 38 samples from the HR- HPV group (22.90%), and the low-grade squamous intraepithelial lesions of the cervix (LSIL) group and the HSIL group had 34 samples (20.48%), respectively. Among the study participants, 65.66% (109/166) were younger than 50, while 34.34% (57/166) were 50 years old and above, with a mean ± standard deviation age of 44.91 ± 12.05 years.

Nearly 94.58% (157/166) of the participants were married, while 5.42% (9/166) were unmarried or had other marital statuses. 71.69% (119/166) of the study participants had given birth vaginally, and 18.67% (31/166) had a caesarean section. In the CC group, there was one patient in whom both delivery methods were used. Approximately 46.99% (78/166) of the women gave birth twice or more. Overall, 74.70% (124/166) of the women were premenopausal, while 25.30% (42/166) of the women were postmenopausal.

Among the patients, 83.13% (138/166) had the negative for intraepithelial lesion or malignancy (NILM) TCT results. None of the TCT results in the samples collected indicated any abnormal glandular epithelial cells. Therefore, 7 (4.22%) and 21 (12.65%) had atypical squamous cells of undetermined significance (ASCUS) and > ASCUS (indicating lesions with a higher degree than ASCUS, including atypical squamous cells cannot exclude high-grade squamous intraepithelial lesions (ASC-H), LSIL, HSIL, and squamous cell carcinoma of the cervix (SCC)) TCT results, separately. A total of 81.33% (135/166) of the patients tested positive for HR-HPV, with the HSIL group having the highest percentage at 100.00% (34/34). About 27.71% (46/166) of the patients were infected with HPV16/18. The CC group had the highest percentage of HPV 16/18 infections, at 73.33% (22/30).

	Characteristics	Value
Age	< 50	109 (65.66%)
	≥ 50	57 (34.34)
Marital status	Married	157 (94.58%)
	Other	9 (5.42%)
Delivery	Eutocia	119 (71.69%)
	Caesarean	31 (18.67%)
	Both	1 (0.60%)
	None	15 (9.04%)
Parity	0	15 (9.04%)
	1	73 (43.97%)
	≧ 2	78 (46.99%)
Menopause	Yes	42 (25.30%)
	No	124 (74.70%)
Cervical cytology	NILM	138 (83.13%)
	ASCUS	7 (4.22%)
	> ASCUS	21 (12.65%)
HR-HPV status	Negative	31 (18.67%)
	Positive	135 (81.33%)
HPV16/18 infection	Negative	120 (72.29%)
	Positive	46 (27.71%)
Pathological grouping	Normal	30 (18.07%)
	HR-HPV	38 (22.90%)
	LSIL	34 (20.48%)
	HSIL	34 (20.48%)
	CC	30 (18.07%)

Table 1. Clinical characteristics of the study population (N = 166). *Abbreviations*: NILM, negative for intraepithelial lesion or malignancy; ASCUS, atypical squamous cells of undetermined significance; HPV, human papillomavirus; LSIL, low-grade squamous intraepithelial lesions of the cervix; HSIL, high-grade squamous intraepithelial lesions of the cervix; CC, cervical cancer; HR-HPV, high-risk human papillomavirus.

CAPZB mRNA levels in cervical lesions of different grades

The expression of CAPZB mRNA in cervical exfoliated cells across various cohorts was assessed using fluorescence in situ hybridization (FISH). The median and interquartile range (IQR) of mean fluorescence intensity (MFI) values were as follows: normal group 30.46 (IQR: 26.39–37.49), HR-HPV group 25.78 (IQR: 20.85–34.60), LSIL group 23.79 (IQR: 20.07–30.85), HSIL group 17.21 (IQR: 14.24–21.73), and CC group 12.62 (IQR: 9.25–16.50) (Table 2). We employed the Kruskal–Wallis H test for our comparison, revealing notable differences in MFI values across five groups ($H = 83.638$, $p = 2.951 \times 10^{-17}$). Following Bonferroni adjustment, we observed that the mRNA expression levels of CAPZB significantly varied among these groups: normal versus HSIL ($p = 2.164 \times 10^{-8}$), normal versus CC ($p = 1.066 \times 10^{-13}$), HR-HPV versus HSIL ($p = 3.300 \times 10^{-5}$), HR-HPV versus CC ($p = 6.577 \times 10–^{10}$), LSIL versus HSIL ($p = 7.496 \times 10^{-3}$), LSIL versus CC ($p = 2.000 \times 10^{-6}$) (Fig. 1a).

However, no significant difference was observed between the normal group and the HR-HPV group ($p = 0.999$), the normal group and the LSIL group ($p = 0.065$), the HR-HPV group and the LSIL group ($p = 1.000$), as well as the HSIL and the CC group ($p = 0.470$) (Fig. 1a). Figure 2a displayed fluorescence images of some samples obtained using a laser confocal microscope.

In the comparisons between the HR-HPV (−) and HR-HPV (+) ($U = 798$, $p = 8.141 \times 10^{-8}$), HPV16/18 (−) and HPV16/18 (+) ($U = 1824$, $p = 7.000 \times 10^{-4}$), and HPV16 (−) and HPV16 (+) groups ($U = 1526$, $p = 0.004$), there were differences in CAPZB mRNA expression, with all p values less than 0.05 (Fig. 1c–e). However, there was no difference in expression between the HPV18 (−) and HPV18 (+) groups ($U = 706$, $p = 0.174$) (Fig. 1f). According to the different cytological results, there was a difference in CAPZB mRNA expression between the NILM, ASCUS and > ASCUS groups ($H = 14.80$, $p = 6.110 \times 10^{-4}$). Significant differences can be seen in the NILM and > ASCUS groups ($p = 1.300 \times 10^{-3}$), but no difference in expression between the NILM and ASCUS groups ($p = 0.201$) or between the ASCUS and > ASCUS groups ($p = 1.000$) (Fig. 1b). Figure 2b and c showed fluorescence images of some samples under a laser confocal microscope.

DNA methylation levels of CAPZB in cervical lesions of different grades

Bisulfite sequencing polymerase chain reaction (BSP) effectively measured the DNA methylation status of CAPZB across various cervical lesions. This assessment uncovered a notable gradient change. The CC group exhibited the highest methylation degree, followed by the HSIL and LSIL groups. Methylation rate (PMR) values showed median percentages of 30.75 (IQR: 22.22–50.00), 25.00 (IQR: 18.45–33.33), and 20.14 (IQR: 13.33–25.42), respectively (Table 2). The Kruskal–Wallis H test indicated significant variations in PMR values among the five groups ($H = 48.334$, $p = 8.041 \times 10^{-10}$). Statistically significant differences emerged in DNA methylation of CAPZB between several groups after the Bonferroni method to adjust for multiple testing. For instance, comparisons included the normal versus HSIL group ($p = 1.570 \times 10^{-4}$) and the normal versus CC group ($p = 1.974 \times 10^{-8}$). The HR-HPV versus HSIL group ($p = 0.011$), and HR-HPV versus CC group ($p = 4.000 \times 10^{-6}$) also showed significant results. Moreover, LSIL versus HSIL ($p = 0.036$) and LSIL versus CC ($p = 2.390 \times 10^{-4}$) comparisons highlighted differences as well (Fig. 3a).

Nevertheless, the analysis revealed no statistically significant differences between the normal and the HR-HPV groups ($p = 1.000$), nor between the normal and the LSIL groups ($p = 0.501$). Lastly, the HR-HPV group and LSIL group ($p = 1.000$), and the HSIL and CC group ($p = 0.620$), all results displayed no significance (Fig. 3a).

Statistical analysis revealed significant differences in the DNA methylation of CAPZB when categorized by HPV typing, specifically HR-HPV (−) and (+) ($U = 3110$, $p = 2.300 \times 10^{-5}$), HPV16/18 (−) and (+) ($U = 3905$, $p = 3.400 \times 10^{-5}$), and HPV16 (−) and (+) ($U = 3145.5$, $p = 2.940 \times 10^{-4}$) as illustrated in Fig. 3c–e. Conversely, no statistically significant differences occurred in comparisons between HPV18 (−) and (+) ($U = 1167.5$, $p = 0.127$) presented in Fig. 3f. Furthermore, no distinctions emerged based on cytology categories ($H = 5.881$, $p = 0.053$) (Fig. 3b).

Comparison of CAPZB mRNA expression and CAPZB DNA methylation as biomarkers

HR-HPV- included the normal group and the HR-HPV group; LSIL+ included the LSIL group, the HSIL group, and the CC group; LSIL− included the normal group, the HR-HPV group, and the LSIL group; HSIL+ included the HSIL group and the CC group; HSIL- included the normal group, the HR-HPV group, the LSIL group and the HSIL group; CC included the CC group only.

Pathological grouping	Case number	FISH		BSP	
		Median (MFI, au)	IQR	Median (PMR, %)	IQR
Normal	30	30.46	26.39–37.49	16.67	8.13–20.21
HR-HPV	38	25.78	20.85–34.60	16.67	12.78–23.33
LSIL	34	23.79	20.07–30.85	20.14	13.33–25.42
HSIL	34	17.21	14.24–21.73	25.00	18.45–33.33
CC	30	12.62	9.25–16.50	30.75	22.22–50.00

Table 2. Detection of CAPZB mRNA and CAPZB DNA methylation in different cervical lesions. *Abbreviations*: HR-HPV, high-risk human papillomavirus; LSIL, low-grade squamous intraepithelial lesions of the cervix; HSIL, high-grade squamous intraepithelial lesions of the cervix; CC, cervical cancer; FISH, fluorescence in situ hybridization; BSP, bisulfite sequencing polymerase chain reaction; IQR, interquartile range; MFI, mean fluorescence intensity; PMR, percentage of methylation rate.

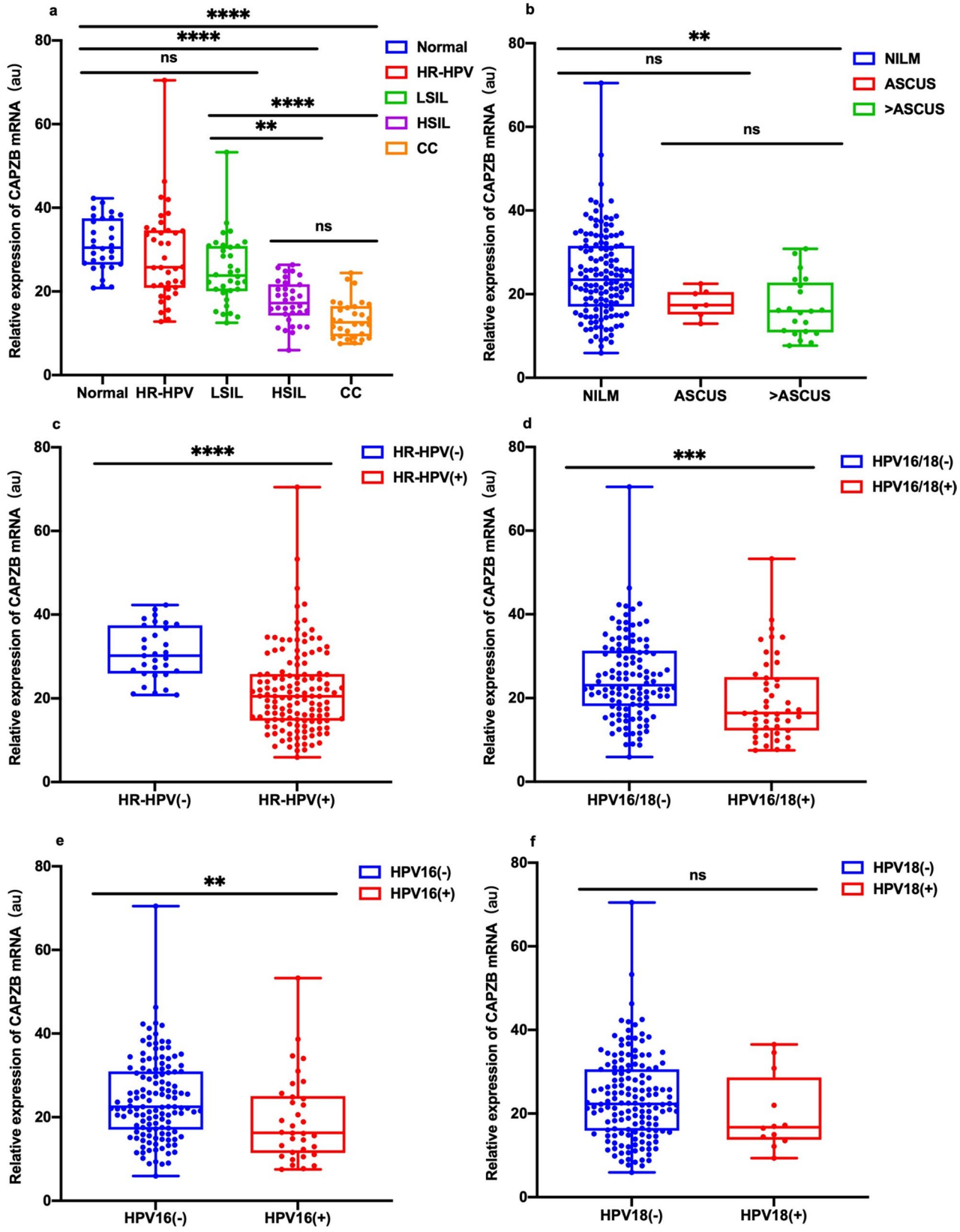
a
****
****
ns
****
**
ns
Normal
HR-HPV
LSIL
HSIL
CC
Relative expression of CAPZB mRNA (au)
0
20
40
60
80
Normal
HR-HPV
LSIL
HSIL
CC
b
**
ns
ns
NILM
ASCUS
>ASCUS
Relative expression of CAPZB mRNA (au)
NILM
ASCUS
>ASCUS
c
****
HR-HPV(-)
HR-HPV(+)
Relative expression of CAPZB mRNA (au)
HR-HPV(-)
HR-HPV(+)
d
***
HPV16/18(-)
HPV16/18(+)
Relative expression of CAPZB mRNA (au)
HPV16/18(-)
HPV16/18(+)
e
**
HPV16(-)
HPV16(+)
Relative expression of CAPZB mRNA (au)
HPV16(-)
HPV16(+)
f
ns
HPV18(-)
HPV18(+)
Relative expression of CAPZB mRNA (au)
HPV18(-)
HPV18(+)

◂**Fig. 1.** Expression of CAPZB mRNA in cervical lesions. (**a**) Expression of CAPZB in different cervical lesions. (**b**) Expression of CAPZB according to cervical cytology. (**c–f**) Expression of CAPZB in different HPV genotypes. Comparisons between two groups were performed using the Mann−Whitney U test, while comparisons between multiple groups were performed using the Kruskal–Wallis H test—the Bonferroni method used for pairwise comparison. ns: $p = 0.05$ or greater; *: $p < 0.05$; **: $p < 0.01$; ***: $p < 0.001$; ****: $p < 0.0001$. A two-sided p value less than 0.05 was considered statistically significant. The upper, middle, and lower lines in the box plots represent the maximum, median, and minimum values, respectively. *Abbreviations:* HPV, human papillomavirus; LSIL, low-grade squamous intraepithelial lesions of the cervix; HSIL, high-grade squamous intraepithelial lesions of the cervix; CC, cervical cancer; NILM, negative for intraepithelial lesion or malignancy; ASCUS, atypical squamous cells of undetermined significance; HR-HPV, high-risk human papillomavirus.

The area under the receiver operating characteristic curve (AUC) values for FISH detection of CAPZB mRNA showed notable discrimination between various histological classifications. Specifically, the AUC values (95% confidence interval, CI) for LSIL+/HR-HPV−, HSIL+/LSIL−, and CC/HSIL− were 0.831 (95% CI 0.770–0.892), 0.893 (95% CI 0.846–0.939),and 0.622 (95% CI 0.503–0.741), separately. Corresponding sensitivities and specificities were 80.61% and 70.59%, 81.25% and 80.39%, 66.67% and 54.69%. The established cut-off value for LSIL+ was 0.512, while HSIL+ and CC cut-offs were 0.616 and 0.214, respectively (Table 3, Fig. 4a).

In contrast, AUC values for BSP detection of CAPZB DNA methylation were lower across groups: 0.744 (95% CI 0.670–0.818), 0.794 (95% CI 0.725–0.863), and 0.587 (95% CI 0.464–0.709). These results indicated sensitivities and specificities varying from 40.00 to 73.47% and 64.71 to 81.37%, accordingly. The cut-off value for LSIL+ was set at 0.382, while HSIL+ and CC reached 0.454 and 0.150, respectively. Full details were presented in Table 3 and Fig. 4b.

In this research, we employed two distinct methodologies to systematically compare the AUC values aimed at differentiating HSIL+ from LSIL−. The results showed a statistically significant difference ($z = 2.315$, $p = 0.021$). Conversely, comparisons of two methods AUC values for LSIL+/HR-HPV− ($z = 1.782$, $p = 0.075$) and CC/HSIL- ($z = 1.552$, $p = 0.121$) did not yield statistical significance. This finding highlighted that FISH detection of CAPZB mRNA excelled in distinguishing HSIL+ from LSIL−. The AUC reached 0.893 with a cut-off value of 0.616. This suggested a potent diagnostic capability as a biomarker.

Discussion

Cervical cancer-related deaths in low- and middle-income countries account for 90% of all deaths related to this disease [22]. To save more lives, it is necessary to conduct timely and accurate screening for high-risk populations, especially those with HSIL [22]. Our study found that CAPZB mRNA is a favorable screening tool for distinguishing HSIL+ from LSIL−.

The CAPZB gene is located on chromosome 1p36.13 and belongs to the F-actin capping protein family [23]. CAPZB is a regulator of actin filament length that determines mitotic cortex thickness during cell cycle progression [24]. Specifically, variations in actin cortex thickness and tension directly influence cell surface tension, thus modulating cell cycle dynamics[24]. In recent years, studies have shown its association with several cancer types. For example, silencing CAPZB in epithelioid sarcoma can inhibit the growth and migration of tumour cells [25]. Feng et al. reported that the rs12045440 polymorphism in the CAPZB intron was significantly associated with the serum TSH concentration in Chinese thyroid tumour patients [26]. A study on liver cancer revealed that HBxΔ3 can increase the invasion and metastasis of liver cancer cells in vivo and in vitro by downregulating CAZPB[27]. These studies revealed the relationships between β subunit genes in the CP and cancer. Moreover, they showed that CAPZB was often deregulated in many malignancies and significantly correlated with metastasis, recurrence and prognosis. CAPZB plays important roles during tumour metastasis by influencing cell morphology, adhesion junctions and migration ability of tumour cells. Another earlier study showed that F-actin capping protein α1 subunit (CAPZA1) gene downregulation in gastric cancer was associated with poor prognosis and increased cancer cell migration and invasion[28].

Nevertheless, in a Japanese study, CAPZB was found to be closely associated with survival outcomes in diffuse large B-cell lymphoma (DLBCL) using a dataset of 470 clinical samples from the publicly available dataset GSE31315[29]. Lowered expression of CAPZB may also increase gamma-delta T cell infiltration and improve prognosis[29]. This was different from previous studies on CAPZB and tumours, which found that reduced CAPZB expression in cancer may promote tumour development and thus reduce survival.

In gynaecological tumours, only Erdogan et al.[12] reported differential methylation of the CAPZB gene in a comparison between ovarian cancer patients and healthy individuals, with ovarian cancer patients being mostly hypermethylated. In addition, the study by Zhao et al. developed a diagnostic model with outstanding performance for endometriosis using machine learning algorithms[30]. The research found that the CAPZB gene has significant diagnostic value, but it has not yet been validated in large-scale clinical trials[30]. Different subunit genes in the CP play important roles in cancer, which is closely related to the role of the CP in controlling cell movement and morphology. Our study is the first to investigate the link between the CAPZB gene and cervical diseases. Perhaps the reduction of the expression of the CAPZB gene contributes to the migration and invasion of cervical cancer cells, and the tumour can progress. Of course, this is our guess, and whether this is the case and whether there is a synergistic effect with HR-HPV infection or even with other genes in this process needs to be confirmed by further research.

The latest screening guidelines mention the potential of methylation and RNA detection studies[4], and an increasing number of studies are being devoted to exploring new biomarkers. In our study, we also investigated the use of CAPZB DNA methylation for distinguishing cervical diseases. Together, for the first time, we explored

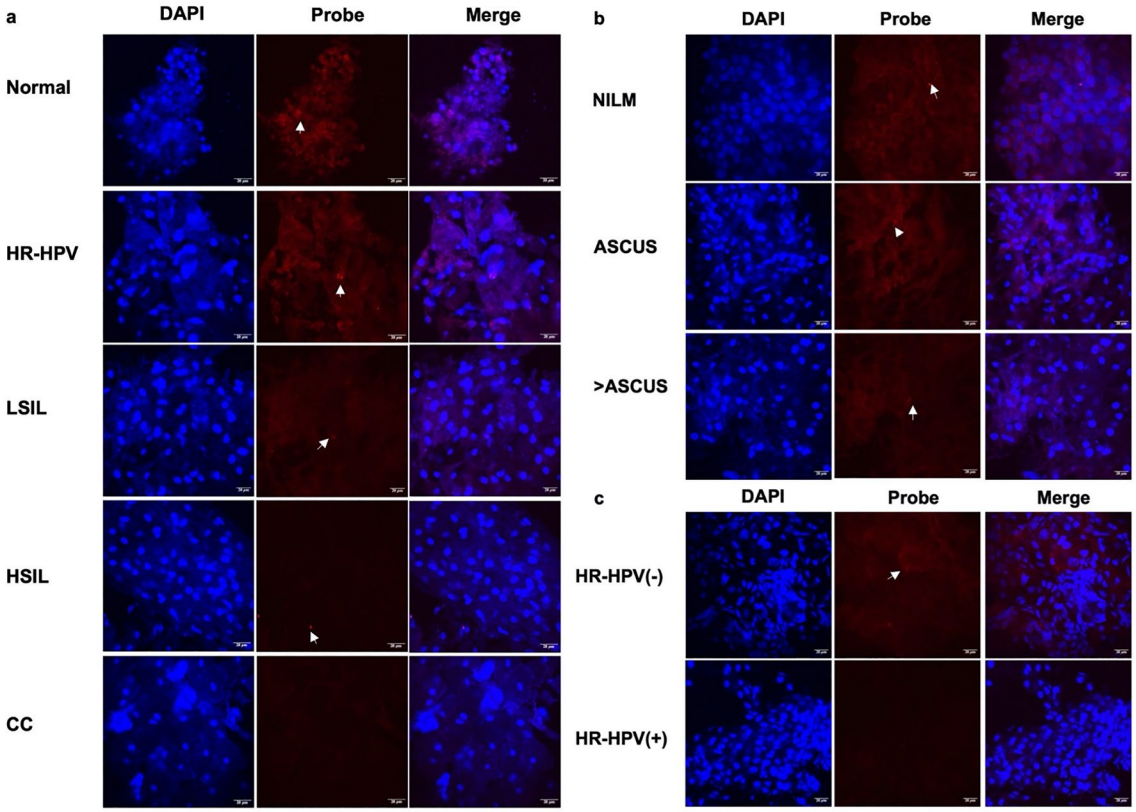

Fig. 2. Fluorescence images of some samples under laser confocal microscopy. (**a**) Fluorescence images of CAPZB expression in samples of different cervical lesions. (**b**) Fluorescence images of CAPZB expression in some samples grouped by cytology. (**c**) Fluorescence images of CAPZB expression in some samples grouped by HR-HPV typing. Scale bar = 20 μm. The white arrows indicated the expression of CAPZB. *Abbreviations*: LSIL, low-grade squamous intraepithelial lesions of the cervix; HSIL, high-grade squamous intraepithelial lesions of the cervix; CC, cervical cancer; NILM, negative for intraepithelial lesion or malignancy; ASCUS, atypical squamous cells of undetermined significance; HR-HPV, high-risk human papillomavirus.

the potential application of a new gene at the mRNA and DNA methylation levels for cervical cancer diagnosis. However, we did not conduct in-depth mechanistic studies on cervical cancer cell lines, which may be our further research plan in the future. In addition, our study also showed that CAPZB mRNA and DNA methylation levels are related to HR-HPV infection.

Compared to DNA, mRNA carries genetic information and can dynamically reflect cell status and regulatory processes. Compared to proteins, mRNA is more sensitive and specific[31]. This may be why many researchers have focused on mRNA. Chen et al. reported that ADCY7 mRNA performs well in distinguishing HPV infection and diagnosing HSIL from LSIL[32]. Duvlis et al. compared HPV E6/E7 mRNA and HPV DNA as screening tools for cervical cancer and reported that the former had advantages such as reducing colposcopy referral rates, decreasing patient anxiety, and lowering the associated costs[33]. Furthermore, a study on oesophageal squamous cell carcinoma(ESCC) tissue revealed that CADM1 mRNA is highly expressed in normal oesophageal tissue and that loss of CADM1 expression affects the invasion and migration of cancer cells[34]. Our study is similar in that we also found that mRNA, as a biomarker, is superior to DNA.

Coppock et al. reported that reclassifying biopsy tissues using HPV RNA in situ hybridization can reduce the overdiagnosis of histological LSIL and can help doctors make better judgements in cases where cytological and histological results are inconsistent[35]. We also applied RNA in situ hybridization techniques, but one of the innovative aspects was the use of fluorescence. FISH techniques were initially used for gene mapping and have advantages such as safety, speed, high sensitivity, long probe preservation time, and the ability to simultaneously display multiple colours, increasing their use in mRNA detection[18,36].

In summary, in this study, for the first time, we investigated the CAPZB gene in cervical lesions and compared the diagnostic value of CAPZB mRNA and CAPZB DNA methylation for cervical lesions. We first demonstrated the potential value of CAPZB mRNA in distinguishing between LSIL− and HSIL+ lesions and used a new FISH technique to detect mRNA, which yielded more direct and clear results. But in fact, our study has several limitations. RNA is prone to degradation and fluorescence attenuation, so fresh samples need to be collected and processed quickly. This requires high-quality cell preservation solutions and immediate experiments with image capture on the same day after collecting each batch of samples, which is time-consuming and labour-intensive.

The BSP technique for methylation analysis also requires considerable time and has complex steps. In addition, our sample size was not sufficient, and future studies with more samples, multiple centres, and multiple perspectives will be needed to verify the diagnostic potential of CAPZB. Despite its limitations, our

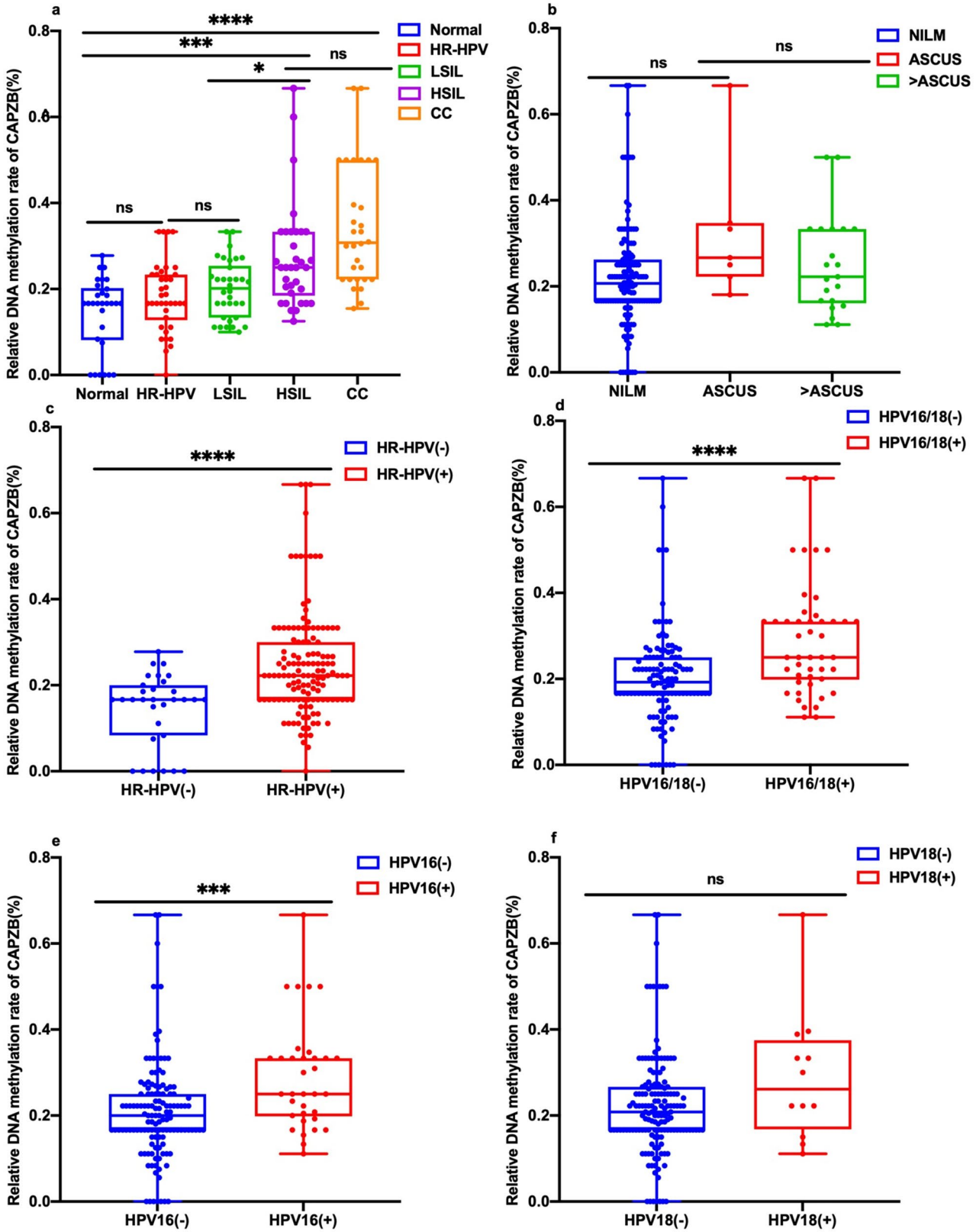

Fig. 3. DNA methylation status of CAPZB in different cervical lesions. (**a**) DNA methylation status of CAPZB in cervical lesions of different grades. (**b**) DNA methylation status of CAPZB according to different cytological results. (**c–f**) DNA methylation status of CAPZB in different HPV genotypes. Comparisons between two groups were performed using the Mann—Whitney U test, while comparisons between multiple groups were performed using the Kruskal–Wallis H test—the Bonferroni method used for pairwise comparison. ns: $p = 0.05$ or greater; *: $p < 0.05$; **: $p < 0.01$; ***: $p < 0.001$; ****: $p < 0.0001$. A two-sided p-value less than 0.05 was considered statistically significant. The upper, middle, and lower lines in the box plots represent the maximum, median, and minimum values, respectively. *Abbreviations*: HPV, human papillomavirus; LSIL, low-grade squamous intraepithelial lesions of the cervix; HSIL, high-grade squamous intraepithelial lesions of the cervix; CC, cervical cancer; NILM, negative for intraepithelial lesion or malignancy; ASCUS, atypical squamous cells of undetermined significance; HR-HPV, high-risk human papillomavirus.

Detection method	Group	Cut-off value	AUC	(95% CI)	Sensitivity (%)	Specificity (%)
FISH	LSIL + /HR-HPV−	0.512	0.831	0.770–0.892	80.61	70.59
	HSIL+/LSIL−	0.616	0.893	0.846–0.939	81.25	80.39
	CC/HSIL-	0.214	0.622	0.503–0.741	66.67	54.69
BSP	LSIL+/HR-HPV−	0.382	0.744	0.670–0.818	73.47	64.71
	HSIL+/LSIL−	0.454	0.794	0.725–0.863	64.06	81.37
	CC/HSIL-	0.150	0.587	0.464–0.709	40.00	75.00

Table 3. AUC values of each detection method. *Abbreviations*: ROC, receiver operating characteristic; AUC, area under the ROC curve; CI, confidence interval; LSIL, low-grade squamous intraepithelial lesions of the cervix; HSIL, high-grade squamous intraepithelial lesions of the cervix; CC, cervical cancer; HR-HPV, high-risk human papillomavirus; FISH, fluorescence in situ hybridization; BSP, bisulfite sequencing polymerase chain reaction. Note: HR-HPV- included the normal group and the HR-HPV group; LSIL+ included the LSIL group, the HSIL group, and the CC group; LSIL− included the normal group, the HR-HPV group, and the LSIL group; HSIL+ included the HSIL group and the CC group; HSIL- included the normal group, the HR-HPV group, the LSIL group and the HSIL group; CC included the CC group only.

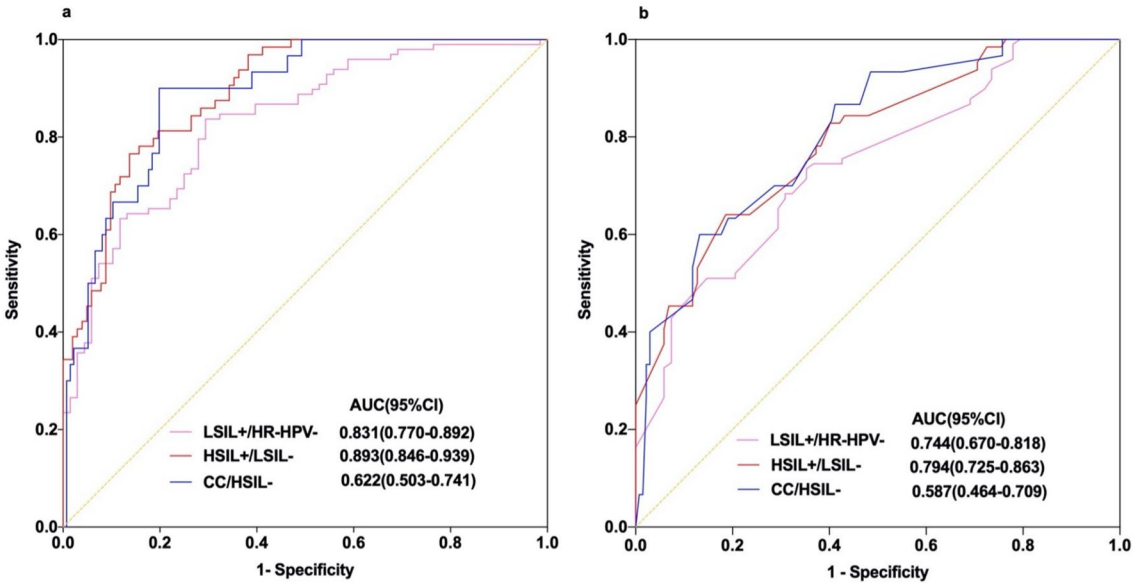

Fig. 4. Comparison of two methods for detecting cervical lesions. (**a**) ROC curve analysis of the FISH method. (**b**) ROC curve analysis of the BSP method. *Abbreviations*: ROC, receiver operating characteristic; AUC, area under the ROC curve; CI, confidence interval; LSIL, low-grade squamous intraepithelial lesions of the cervix; HSIL, high-grade squamous intraepithelial lesions of the cervix; CC, cervical cancer; HR-HPV, high-risk human papillomavirus; FISH, fluorescence in situ hybridization; BSP, bisulfite sequencing polymerase chain reaction. Note: HR-HPV- included the normal group and the HR-HPV group; LSIL+ included the LSIL group, the HSIL group, and the CC group; LSIL− included the normal group, the HR-HPV group, and the LSIL group; HSIL+ included the HSIL group and the CC group; HSIL- included the normal group, the HR-HPV group, the LSIL group and the HSIL group; CC included the CC group only.

study identified another new gene for cervical lesion screening, providing a new perspective and achieving a breakthrough in the precise screening for HSIL. Our study is meaningful and promising. Furthermore, we will assess CAPZB gene expression in various cervical lesion tissues and further explore the mechanisms by which CAPZB contributes to the development and progression of cervical cancer and its precancerous lesions in subsequent research, thereby providing a theoretical basis for the precise screening of cervical lesions.

Conclusion

This study revealed that the level of CAPZB mRNA can serve as a suitable biomarker to differentiate between LSIL− and HSIL+ and performs better than CAPZB DNA methylation in terms of discriminatory ability. The level of CAPZB mRNA may serve as an auxiliary indicator for HR-HPV infection. These findings provide valuable research directions for exploring therapeutic targets for cervical cancer and preventing sustained HR-HPV infection.

Materials and methods

Ethical statement

This study was approved by the Ethics Committee of Minhang Hospital, affiliated with Fudan University (approval number: 2022-Approval-019-01K). Written informed consent was obtained from all patients participating in the study. Our study was performed in accordance with the Declaration of Helsinki. All experiments were performed in accordance with relevant named guidelines and regulations.

Study subjects and selection

A total of 465 cervical exfoliated cell samples from female patients were collected from December 2022 to April 2023 at the Department of Gynaecology, Minhang Hospital, affiliated with Fudan University. The collected data encompassed name, age, marital status, mode of delivery, number of deliveries, menopausal status, TCT results, HR-HPV typing results, routine vaginal discharge results, surgical method, colposcopy examination results, and histopathological examination results were recorded.

The inclusion criteria were as follows: aged 20 years or older and had a history of sexual activity. Exclusion criteria: Previously treated for gynaecological tumours; acute vaginal inflammation; acute or chronic systemic diseases; insufficient or poor-quality cell samples; and incomplete clinical data.

Therefore, there were 299 non-compliant samples, the details were as follows: 109 cases of vaginal inflammation (pseudomycosis of the vulva and vagina in 78 patients, bacterial vaginosis in 5 patients, trichomonas vaginitis in 1 patient, and nonspecific vaginitis in 25 patients), 43 cases of no examination results (only lack of routine vaginal discharge examination in 20 patients, lack of TCT examination in 20 patients, lack of HR-HPV testing in 2 patients, and absence of all three in 1 patient), 87 cases of sample quality issues (insufficient cell quantity or poor quality), and 60 cases of other sample quality issues.

The study ultimately comprised 166 samples, as illustrated in Fig. 5. Histopathological analysis categorized the samples into five distinct groups. The normal group included patients with regular vaginal leucorrhea and TCT results, alongside HR-HPV typing negative results that required no histopathological examination. The HR-HPV group involved individuals with normal leucorrhea and TCT findings but tested positive for HR-HPV typing. These patients underwent colposcopy and cervical biopsy, revealing no cervical lesions. The remaining categories included the LSIL group, the HSIL group, and the CC group, defined by the highest-grade lesions identified from cervical tissue biopsy, cervical cone biopsy, or comprehensive hysterectomy.

Sample processing

Approximately 10 mL of the samples stored in TCT bottles were centrifuged at 1500 rpm for 10 min. After centrifugation, the supernatant was discarded, and the remaining cell pellet was mixed and divided into two portions, each placed in a 1.5 mL centrifuge tube and stored at −80 °C for subsequent experiments. One portion of the sample was subjected to FISH, and the other portion was subjected to BSP after bisulfite modification.

Thin-Prep cytology test (TCT)

This study employed liquid-based cytology technology from Hologic company. TCT-specific cell brushes collected samples efficiently. In the cytology slide preparation room, glass slides with cervical exfoliated cells and preservative solution entered an automated system. This system utilized the thin-layer liquid-based cytology method for processing. Highly experienced pathologists reviewed the resulting slides. The TCT diagnostic reports followed the 2014 version of the Bethesda system (TBS)[37].

The TCT results for the 166 samples in this study revealed no abnormal glandular epithelial cells. Consequently, we classified the TCT results into three distinct categories for further analysis: NILM, ASCUS, and > ASCUS. The > ASCUS category encompassed lesions indicating a higher degree than ASCUS, which included ASC-H, LSIL, HSIL, and SCC.

High-risk human papillomavirus (HR-HPV) test

The study employed the Roche Cobas 4800 HPV DNA test for HPV detection. This test, approved by the American Food and Drug Administration (FDA), identified 14 high-risk HPV types. It included HPV16, HPV18, and others. The detection distinguished HPV16 and HPV18 as individual positive or negative results. In contrast, the remaining 12 types yielded a collective positive result without additional subtype classification. Cervical exfoliated cells were gathered using a specialized HPV collection brush, adhering strictly to reagent kit guidelines.

The analysis of 166 samples led to comparisons across various HR-HPV groupings, including HR-HPV (−) versus HR-HPV (+), HPV16/18 (−) versus HPV16/18 (+), and similar pairings for HPV16 and HPV18.

Bisulfite sequencing polymerase chain reaction (BSP)

A genomic DNA extraction kit (Tiangen, DP304-03, Shanghai, China) was used to extract gDNA from all cell samples, and an EZ DNA Methylation-Gold Kit (Zymo, D5006, USA) was used for bisulfite conversion. Two microlitres of bisulfite-modified DNA from each sample was subjected to PCR in a 50 μL reaction system using the CAPZB methylation primer (Sangon Biotech, Shanghai, China). The reaction mixture was preheated at 95 °C for 5 min and then subjected to PCR amplification (10 s at 98 °C, 30 s at 55 °C, and 30 s at 72 °C for a total of 35 cycles, followed by a 5 min extension at 72 °C). The PCR products were stored at 4 °C. The PCR products were cloned and inserted into the pEASY®-T vector (TransGen Biotech, CT101-02, Beijing, China), and 10 or more clones were selected from each sample for PCR amplification using M13 primers (Sangon Biotech) and subsequent identification. Positive clones were then subjected to sequencing analysis. The primer sequences can be found in Table 4.

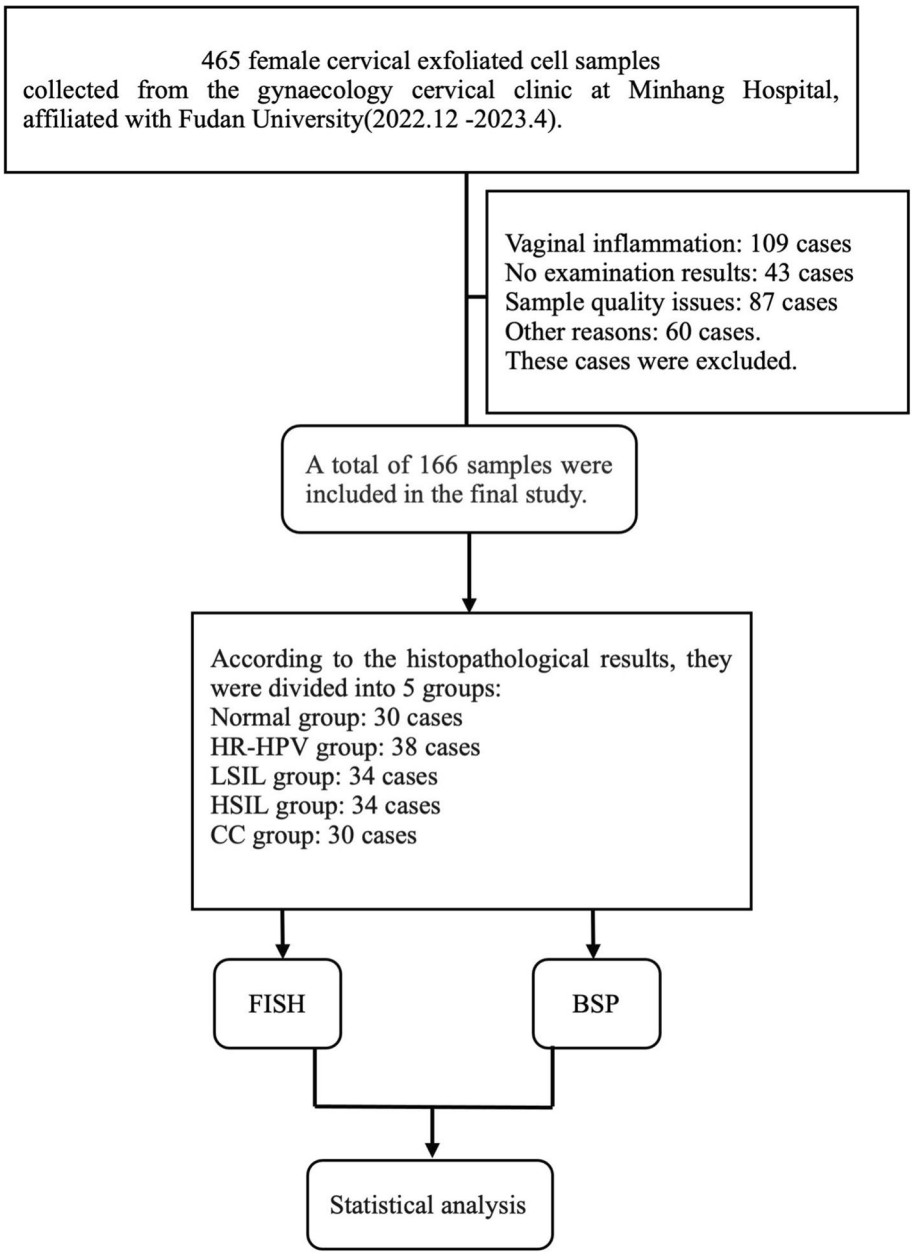

Fig. 5. Study flowchart. *Abbreviations*: HR-HPV, high-risk human papillomavirus; LSIL, low-grade squamous intraepithelial lesions of the cervix; HSIL, high-grade squamous intraepithelial lesions of the cervix; CC, cervical cancer. FISH, fluorescence in situ hybridization; BSP, bisulfite sequencing polymerase chain reaction.

Gene	Primer	Sequence (5′–3′)	Product size
CAPZB	Forwards	GATTTTGGTTTATTGTAATTTTTGTTTT	155 bp
	Reverse	AAACCATCCTAACCAACATAATAAAACC	
M13	Forwards	GTTGTAAAACGACGGCCAG	354 bp
	Reverse	CAGGAAACAGCTATGAC	

Table 4. Primer sequences for the methylation reaction.

The CPRZB gene PMR was the percentage of methylated sites relative to the number of CG sites obtained from all clones sequenced in each cervical cell sample.

Fluorescence in situ hybridization (FISH)

FISH was performed using a CAPZB probe (LGC, USA) and SMF series reagents (LGC) according to the manufacturer's instructions. Pretreatment: After centrifuging the cells at 1500 rpm for 2 min, the supernatant was discarded, the cells were mixed with 1 mL of 1× PBS, and the supernatant was discarded after centrifugation. The samples were mixed with 1 mL of fixation buffer (made with methanol and glacial acetic acid at a 3:1 ratio) and incubated at room temperature for 10 min. The supernatant was discarded after centrifugation, the samples were washed 3 times with 1 mL of 1 × PBS, and the supernatant was discarded after centrifugation. The mixture was resuspended in 1 mL of 70% ethanol and incubated at 4 °C for at least 1 h. Hybridization: The supernatant was discarded after centrifugation, 500 μL of washing buffer A (SMF-WA1-60, LGC) was added, and the supernatant was discarded after centrifugation. The cells were resuspended in hybridization buffer containing 100 μL of CAPZB probe and incubated at 37 °C for 16 h in the dark. Approximately 50% of the hybridization buffer containing the probe was discarded after centrifugation, 500 μL of washing buffer A was added, the supernatant was discarded after centrifugation, and the samples were resuspended in 500 μL of washing buffer A and incubated at 37 °C for 30 min in the dark. After centrifugation, the supernatant was discarded, and the cells were resuspended in 500 μL of DAPI nuclear stain (5 ng/mL) and incubated at 37 °C for 30 min in the dark. After centrifugation, the supernatant was discarded, and the sample was resuspended in 500 μL of washing buffer B (SMF-WB1-20, LGC). After centrifugation, the supernatant was discarded, and the sample was mixed with 20 μL of anti-fading sealant, which was then placed on a glass slide, covered with a coverslip and sealed with nail polish. The slide was placed with the cover slip facing down, and immersion oil was added. Images were obtained under a fluorescence confocal microscope (Nikon, Shanghai, China) using the 408 nm DAPI and 561 nm TRITC channels.

Quantification of probe fluorescence intensity in cell nuclei was performed using ImageJ version 2.3.0 software (National Institutes of Health, USA). The format of the confocal images was converted to grayscale, and the ROI (region of interest) Manager interface was used to outline 10 or more cell nuclei and 3 background regions using the selection tool. The relevant values were obtained through measurement. For a single-channel fluorescence image, each pixel grayscale value represented the fluorescence intensity at that point, and the MFI was calculated as follows: MFI = Mean (nucleus) = Corrected cumulated optical density (IntDen)(nucleus)/Area (nucleus) = IntDen (nucleus)/Area (nucleus) − Mean (background). IntDen = Mean × Area.

Statistical analysis

All statistical analyses were performed with IBM SPSS version 29.0 software (IBM Corporation, New York, USA). Plotting was achieved using GraphPad Prism version 10.0 software (GraphPad Software Company, San Diego, USA). Data underwent evaluation for normality through the Shapiro–Wilk test, alongside Levene's test for assessing the homogeneity of the variance. Continuous data were expressed with median and IQR, while categorical variables were represented as component ratios (percentages). We utilized the Mann–Whitney U test to compare independent samples from two groups. For multiple independent group samples, we employed the Kruskal–Wallis H test. We performed post hoc comparisons using the Bonferroni method to adjust for multiple testing.

Receiver operating characteristic (ROC) curve analysis was completed with histopathological results as the gold standard for calculating AUC. The Youden index was used to determine the optimal cut-off value, which provided corresponding sensitivity and specificity. DeLong's test was used to compare the AUC values of the two ROC curves. This method allowed for the comparison of the effectiveness of CAPZB mRNA and DNA methylation as biomarkers in cervical exfoliated cells. A two-sided p-value less than 0.05 was considered statistically significant.

Data availability

All the data generated or analysed during this study are included in this article. Further enquiries can be redirected to the corresponding author.

Received: 27 February 2024; Accepted: 26 August 2024
Published online: 29 August 2024

References

1. Bray, F. *et al.* Global cancer statistics 2022: GLOBOCAN estimates of incidence and mortality worldwide for 36 cancers in 185 countries. *CA. Cancer J. Clin.* **74**, 229–263 (2024).
2. Han, B. *et al.* Cancer incidence and mortality in China, 2022. *J. Natl. Cancer Cent.* **4**, 47–53 (2024).
3. McBride, A. A. Human papillomaviruses: Diversity, infection and host interactions. *Nat. Rev. Microbiol.* **20**, 95–108 (2022).
4. Cao, M. *et al.* Cancer screening in China: The current status, challenges, and suggestions. *Cancer Lett.* **506**, 120–127 (2021).
5. Swid, M. A. & Monaco, S. E. Should screening for cervical cancer go to primary human papillomavirus testing and eliminate cytology?. *Mod. Pathol.* **35**, 858–864 (2022).
6. Banerjee, D., Mittal, S., Mandal, R. & Basu, P. Screening technologies for cervical cancer: Overview. *CytoJournal.* **19**, 23 (2022).
7. Li, Y. Modern epigenetics methods in biological research. *Methods San Diego Calif.* **187**, 104–113 (2021).
8. Senga, S. S. & Grose, R. P. Hallmarks of cancer-the new testament. *Open Biol.* **11**, 200358 (2021).
9. Wang, D. *et al.* Capping protein regulates endosomal trafficking by controlling F-actin density around endocytic vesicles and recruiting RAB5 effectors. *eLife.* **10**, e65910 (2021).
10. Santio, N. M. *et al.* PIM1 accelerates prostate cancer cell motility by phosphorylating actin capping proteins. *CCS.* **18**, 121 (2020).

11. Das, J. K., Roy, S. & Guzzi, P. H. Analyzing host-viral interactome of SARS-CoV-2 for identifying vulnerable host proteins during COVID-19 pathogenesis. *Infect. Genet. Evol.* **93**, 104921 (2021).
12. Erdogan, O. S. *et al.* Genome-wide methylation profiles in monozygotic twins with discordance for ovarian carcinoma. *Oncol. Lett.* **20**, 357 (2020).
13. Brhane, Y. *et al.* Genetic determinants of lung cancer prognosis in never smokers: A pooled analysis in the international lung cancer consortium. *Cancer Epidemiol. Biomark. Prev.* **29**, 1983–1992 (2020).
14. Bastrup, J. *et al.* Anti-Aβ antibody aducanumab regulates the proteome of senile plaques and closely surrounding tissue in a transgenic mouse model of Alzheimer's disease. *J. Alzheimers Dis.* **79**, 249–265 (2021).
15. Šestáková, Š, Šálek, C. & Remešová, H. DNA methylation validation methods: A coherent review with practical comparison. *Biol. Proced.* **21**, 19 (2019).
16. Singer, B. D. A practical guide to the measurement and analysis of DNA methylation. *Am. J. Respir. Cell Mol. Biol.* **61**, 417–428 (2019).
17. Constâncio, V., Nunes, S. P., Henrique, R. & Jerónimo, C. DNA methylation-based testing in liquid biopsies as detection and prognostic biomarkers for the four major cancer types. *Cells* **9**, 624 (2020).
18. Young, A. P., Jackson, D. J. & Wyeth, R. C. A technical review and guide to RNA fluorescence in situ hybridization. *PeerJ.* **8**, e8806 (2020).
19. Zheng, Y. *et al.* The role of mRNA in the development, diagnosis, treatment and prognosis of neural tumors. *Mol. Cancer.* **20**, 49 (2021).
20. Ariston Gabriel, A. N. *et al.* The involvement of exosomes in the diagnosis and treatment of pancreatic cancer. *Mol. Cancer.* **19**, 132 (2020).
21. Xu, Y. *et al.* The expression of HPV E6/E7 mRNA in situ hybridization in HPV typing-negative cervical cancer. *Int. J. Gynecol. Pathol.* **42**, 11–20 (2023).
22. Suba, E. J. *et al.* WHO should adjust its global strategy for cervical cancer prevention. *BMJ Glob. Health.* **8**, e012031 (2023).
23. Maruyama, K. & Kawamura, M. Effect of H-meromyosin and beta-actinin on the particle length of F-actin. *J. Biochem.* **64**, 263–265 (1968).
24. Chugh, P. *et al.* Actin cortex architecture regulates cell surface tension. *Nat. Cell Biol.* **19**, 689–697 (2017).
25. Mukaihara, K. *et al.* Expression of F-actin-capping protein subunit beta, CAPZB, is associated with cell growth and motility in epithelioid sarcoma. *BMC Cancer.* **16**, 206 (2016).
26. Feng, S. *et al.* Association between rs12045440 polymorphism in the CAPZB intron and serum TSH concentrations in Chinese thyroid tumor patients. *Int. J. Endocrinol.* **2015**, 250542 (2015).
27. Li, W. *et al.* Carboxyl-terminal truncated HBx contributes to invasion and metastasis via deregulating metastasis suppressors in hepatocellular carcinoma. *Oncotarget.* **7**, 55110–55127 (2016).
28. Lee, Y.-J. *et al.* Prognostic value of CAPZA1 overexpression in gastric cancer. *Int. J. Oncol.* **42**, 1569–1577 (2013).
29. Wang, Y., Tsukamoto, Y., Hori, M. & Iha, H. Disulfidptosis: A novel prognostic criterion and potential treatment strategy for diffuse large B-cell lymphoma (DLBCL). *Int. J. Mol. Sci.* **25**, 7156 (2024).
30. Zhao, X. *et al.* Unraveling pathogenesis, biomarkers and potential therapeutic agents for endometriosis associated with disulfidptosis based on bioinformatics analysis, machine learning and experiment validation. *J. Biol. Eng.* **18**, 42 (2024).
31. Xi, X. *et al.* RNA Biomarkers: Frontier of precision medicine for cancer. *Non-Coding RNA.* **3**, 9 (2017).
32. Li, X. *et al.* Promoter hypermethylation of SOX11 promotes the progression of cervical cancer in vitro and in vivo. *Oncol. Rep.* **41**, 2351–2360 (2019).
33. Duvlis, S. *et al.* HPV E6/E7 mRNA versus HPV DNA biomarker in cervical cancer screening of a group of Macedonian women. *J. Med. Virol.* **87**, 1578–1586 (2015).
34. Qian, J. B. *et al.* CADM1 mRNA expression and clinicopathological significance in esophageal squamous cell carcinoma tissue. *Genet. Mol. Res.* **16**, (2017).
35. Coppock, J. D., Willis, B. C., Stoler, M. H. & Mills, A. M. HPV RNA in situ hybridization can inform cervical cytology-histology correlation. *Cancer Cytopathol.* **126**, 533–540 (2018).
36. Rensen, E. *et al.* Sensitive visualization of SARS-CoV-2 RNA with CoronaFISH. *Life Sci. Alliance.* **5**, e202101124 (2022).
37. Pangarkar, M. A. The Bethesda system for reporting cervical cytology. *CytoJournal.* **19**, 28 (2022).

Author contributions

X.C. conceived, designed, and conducted the experiments, collected and analysed the data, and drafted the manuscript. W.Q.H. and J.H. provided guidance on the project and experiments. X.X.Z., Z.Y.X., and L.F.W. participated in sample collection. L.X. contributed to the project design, research supervision, and manuscript content revisions. All the authors have read and approved the final manuscript.

Funding

This work was generously supported by grants from Hospital-level Disciplines-Chronic Disease Group-Cervical Diagnosis and Treatment Centre and Obstetrics Endocrinology (YJXK-2021-11).

Competing interests

The authors declare no competing interests.

Additional information

Correspondence and requests for materials should be addressed to L.X.